Available online at www.sciencedirect.com
ScienceDirect
European Journal of Pharmaceutics and Biopharmaceutics 69 (2008) 417–425
European Journal of Pharmaceutics and Biopharmaceutics
www.elsevier.com/locate/ejpb

Research paper

# Self-assembled polyelectrolyte nanocomplexes between chitosan derivatives and enoxaparin

Wei Sun [a], Shirui Mao [a,*], Dan Mei [a], Thomas Kissel [b]

[a] Shenyang Pharmaceutical University, Shenyang, China
[b] Department of Pharmaceutics and Biopharmacy, Philipps-University Marburg, Marburg, Germany

Received 25 October 2007; accepted in revised form 7 January 2008
Available online 26 January 2008

**Abstract**

Polyelectrolyte complexes (PEC) formed from chitosan derivatives and enoxaparin were prepared and parameters influencing complex formation were characterized. Dynamic light scattering (DLS) and laser doppler anemometry (LDA) were used to study the complexation process. Surface morphology of the PECs was observed with atomic force microscopy (AFM). The PEC formation process was influenced by a variety of parameters, including the system pH, polymer/enoxaparin mass ratio, polymer molecular weight, concentration and structure. Soluble complexes in the size range of 200–500 nm with spherical morphology could be obtained at optimized polymer/enoxaparin ratios in the pH range of 3.0–6.5, with positive charge and drug encapsulation efficiency of approximately 90%. An increase in ionic strength of the medium accelerated the dissociation of chitosan/enoxaparin complexes. In contrast, chitosan thiolation, methylation and PEGylation significantly improved the stability of the complexes. Physicochemical properties of the PECs, including particle size, charge density and morphology, could be modified by using different chitosan derivatives. On the basis of our results, we suggest that interactions involved in PEC formation were partly electrostatic in nature, involving the positively charged chitosan derivatives and the negatively charged enoxaparin at pH values in the vicinity of the p$K_a$ interval of the two polymers. Oral absorption of the polyelectrolyte nanocomplexes will be studied in vivo.


*Keywords:* Chitosan; Thiolated chitosan; Trimethyl chitosan; PEGylation; LMWH; Enoxaparin; Polyelectrolyte complexes; Nanoparticle

## 1. Introduction

Heparin is a glycosaminoglycan used mainly as an anticoagulant for the prevention of venous thrombosis and pulmonary embolism in patients undergoing surgery [1]. In the last years, low molecular weight heparin (LMWH) has replaced unfractionated heparin (UH) in many countries mainly due to its longer half-life and less bleeding [2]. Nevertheless, presumably because of the relatively large size and strong negative charge, LMWH still exhibits poor oral bioavailability and consequently has to be administered via the parenteral route. Various attempts have been reported to attain better oral bioavailability, including lipidization of heparin or coadministration with penetration enhancers [3–5], but have met with limited success. More recently, Hoffart et al. reported that a new oral polymeric nanoparticle delivery system of LMWH showed promising absolute bioavailability of more than 51% by a combination of nanoparticle system and mucoadhesive properties of polymers used [6].

Indeed, nanoparticle delivery system, which is shown to protect peptide drugs from degradation in the GI tract and increase the intimacy of contact between drug and mucus membrane at the absorption sites hence improve their bioavailability, has increasingly been investigated these years as a carrier for hydrophilic macromolecular drugs to improve their stability and permit administration through

* Corresponding author. School of Pharmacy, Shenyang Pharmaceutical University, 103, Wenhua Road, #32, Shenyang 110016, China. Tel./fax: +86 24 23986358.
*E-mail address:* shiruimao156@hotmail.com (S. Mao).

0939-6411/$ - see front matter © 2008 Elsevier B.V. All rights reserved.
doi:10.1016/j.ejpb.2008.01.016

nonparenteral routes. Although a wide variety of techniques are available for producing nanoparticles including solvent evaporation, interfacial polymerization and emulsion polymerization methods, most of these approaches involve the use of organic solvents, heat or vigorous agitation, procedures which are potentially harmful to sensitive biomolecules. In recent years, self-assembly of proteins with natural or synthetic polyelectrolytes to form complexes (polyelectrolyte complex, PEC) with drug candidates has drawn increasing attention [7]. PEC formation leads to particles with dimensions on a colloidal level, generating optically homogeneous and stable nano-dispersions. In addition, such methods have the advantage of not necessitating sonication and organic solvents during preparation, therefore minimizing possible damage to drug candidates.

A critical parameter influencing properties of nanoparticle delivery system is the characteristics of the polymer employed [8]. Chitosan (CS) is a nontoxic, bioadhesive and biocompatible cationic polysaccharide produced by partial deacetylation of chitin isolated from naturally occurring crustacean shells. Its inherent bioadhesive nature and the capacity to open the tight junctions in the mucosa have been reported [9,10]. Due to its specific properties, chitosan has found a number of applications in drug delivery including that of an absorption enhancer of hydrophilic macromolecular drugs and as gene delivery system [11]. The application of chitosan in the biomedical field is limited, however, by its poor solubility in physiological media. Chitosan is only soluble in aqueous acidic solution below pH 6.5, in which the primary amino groups of chitosan are protonated. To further improve the poor water solubility of chitosan and its mucoadhesiveness, various chitosan derivatives were developed, such as trimethyl chitosan (TMC), PEGylated TMC copolymers and thiolated chitosans [12,13]. These chitosan derivatives have shown promising characteristics in the development of drug delivery systems and especially in that of polymeric nanoparticle delivery system [14,15].

Enoxaparin is a medicine known as a low molecular weight heparin. It is a highly acidic mucopolysaccharide formed of equal parts of sulfated D-glucosamine and D-glucuronic acid with sulfaminic bridges. Enoxaparin is a well known and commonly used anticoagulant which has antithrombotic properties. We noticed that chitosan is positively charged at pH $< 6.5$ due to the protonation of the amino groups and enoxaparin is negatively charged. Therefore, electrostatic interactions between both entities can be used as a driving force for PEC formation. Although Kikuchi mentioned that heparin seemed to precipitate when interacting with chitosan [16], our recent study demonstrated that stable PECs could be formed between chitosan derivatives and enoxaparin in the pH range of 3.0–6.5, with particle size in the range of 200–500 nm and drug encapsulation efficiency approximately 90%. This approach has not been investigated systemically to the best of our knowledge. In the present work, the feasibility of PEC formation between enoxaparin and various chitosan derivatives by self-assembly was evaluated. The properties of soluble PECs were characterized in terms of particle size, zeta potential, morphology and encapsulation efficiency. Various factors influencing the PEC formation process were investigated in detail. Influences of polymer structure on the properties of the nanocomplexes were discussed.

## 2. Materials and methods

### 2.1. Materials

Chitosan (400 kDa) was purchased from Weifang Kehai Chitin Co., Ltd. (China) with a degree of deacetylation (DD) of 86.5%. Enoxaparin (mean MW 4500 Da) was kindly provided as a gift by Dongying Tiandong Biochemical Co. Ltd. (China). L-Cysteine was purchased from Beijing Solarbio Science and Technology Co., Ltd. (Beijing, China). 1-Ethyl-3-(3-dimethylaminopropyl) carbodiimide hydrochloride (EDAC) and *N*-Hydroxysuccinimide (NHS) were purchased from Shanghai Medpep Co., Ltd. (Shanghai, China). All other chemicals were of analytical grade.

### 2.2. Chitosan derivatives preparation and characterization

Chitosans of different molecular weights were prepared by depolymerization as described previously [17], and the obtained polymers were nominated based on their molecular weight. For example, chitosan with molecular weight of 400 kDa is abbreviated as CS 400, the same as for the other polymers. Trimethyl chitosan (TMC) derivatives were prepared according to a two-step method described previously with a quaternization degree of 40% [18]. Grafting of TMC with poly (ethylene glycol) 5 kDa was achieved to yield copolymers PEG(5)$_{19}$-g-TMC(50) as described elsewhere [13]. The following nomenclature was adopted for the copolymers: PEG($X$)$_n$-g-TMC(50), where $X$ denotes the molecular weight of PEG in kDa and the subscript $n$ represents the average number of PEG chains per TMC macromolecule of 50 kDa. Thiolated chitosans were synthesized according to a method reported previously with little modification [19]. Briefly, cysteine was covalently attached to chitosan via the formation of an amide bond mediated by carbodiimide and *N*-hydroxysuccinimide to obtain chitosan–cysteine conjugates. Iodine titration was used to determine the thiol-group content.

### 2.3. Preparation of CS/enoxaparin nanocomplexes

CS/enoxaparin PECs were prepared from positively charged chitosan and negatively charged enoxaparin by self-assembly. Briefly, chitosan solutions of varied concentration (as indicated below) were prepared by dissolving chitosan powder in 0.25% acetic acid solution and filtered through a Millipore Millex 0.45 μm filter. Enoxaparin dissolved in distilled water (0.5 mg/ml) was added into the chitosan solution under magnetic stirring. The system pH

was adjusted with 1 N HCl or 1 N NaOH as required and then incubated for further 0.5 h at room temperature. All experiments were performed in triplicate at ambient temperature. Freshly prepared solutions were used in each experiment.

### 2.4. Dynamic light scattering (DLS)

Measurements of particle size were carried out using a Zetasizer 4 (Malvern Instruments, Herrenberg, Germany). Scattering light was detected at 90° angle at a temperature of 25 °C. For data analysis, the viscosity (0.88 mPa·s) and the refractive index (1.33) of distilled water at 25 °C were used. Kcps (kilo count per second), which is the intensity of the light scattering signal measured in count/s, was noted during the measurements and has been demonstrated to be able to be used as a measure of particle concentration in a sample [7]. Measurements were analyzed using the CONTIN algorithm. Particle sizes of PECs were given as means ± SD ($n = 3$) from three samples.

### 2.5. Laser doppler anemometry (LDA)

The zeta potential measurements of the PECs were carried out in the standard capillary electrophoresis cell of a Zetasizer 4 (Malvern Instruments, Herrenberg, Germany) at 25 °C. Zeta potential of samples is expressed as mean ± SD ($n = 3$).

### 2.6. Enoxaparin encapsulation efficiency

The amount of enoxaparin entrapped in PEC was calculated by measuring the difference between the total amount of enoxaparin added to the solution and the quantity of free enoxaparin remaining in the aqueous supernatant after the PEC formation. For this purpose, PECs were centrifuged at 20,000 rpm/min for 1 h at room temperature. The quantity of enoxaparin in the supernatant was determined with Azure II colorimetric method [20]. The drug encapsulation efficiency was expressed as the percentage of enoxaparin entrapped with respect to the initial value. All samples were measured in triplicate.

### 2.7. Morphology of the complexes

Atomic force microscopy was employed to characterize the morphology of PECs using a PicoPlus AFM (Agilent Technologies, Tempe, AZ, USA). The samples were diluted with ultra pure water and 10 μl of the diluted sample was applied to a freshly cleaved mica surface and allowed to adhere to the surface for a few minutes. The samples were allowed to air-dry (ca. 10 min). Commercially available silicon tips attached to I-type silicon cantilevers with a length of 230 μm, a resonance frequency of about 140 kHz and a scan frequency of 0.8–1.1 Hz were used. All measurements were performed in tapping mode in order to avoid damage of the sample surface.

### 2.8. Statistical analysis

Results are depicted as means ± SD from at least three measurements. Significance between the mean values was analyzed by one-way ANOVA with the post hoc Scheffe test (SPSS 11.0, SPSS Inc., Chicago, IL, USA). Differences were considered to be significant at a level of $p < 0.05$.

## 3. Results and discussion

### 3.1. Chitosan modification and characterization

It has been reported that the molecular weight of chitosan influenced the stability of the biomolecule/chitosan complex, the efficiency of cell uptake once in contact with the cellular membrane and the dissociation of active molecule from the complex after subsequent endocytosis [21], therefore, it is essential to elucidate the influence of chitosan molecule weight on the properties of the complex. For this purpose, chitosans with molecular weights of 400, 100, 50 and 10 kDa were prepared, respectively, using the oxidative degradation method [17]. As shown in Table 1, the actual molecular weights of the produced chitosans were in good agreement with the expected values without modifying the degree of deacetylation.

In order to further improve the mucoadhesion of chitosan, thiolated chitosan derivatives were developed. Compared to unmodified chitosan, thiolated chitosans have significantly improved mucoadhesiveness and permeation-enhancing capacity owing to the formation of covalent bonds between thiol groups of the polymer and cysteine-rich subdomains of glycoproteins in the mucus [22]. While the thiol-group content could potentially influence the characteristics of polymer and therefore properties of the complex, chitosan–cysteine conjugates with two degrees of thiolation, 49.5 μmol/g and 151.2 μmol/g, respectively, were prepared for the following investigations.

While chitosan is only soluble in acidic environment, *N*-trimethyl chitosan chloride (TMC), a quaternized chitosan derivative, was synthesized to further enhance its solubility. TMC has perfect solubility in water over a wide pH range and shows absorption-enhancing effects even in neutral and basic pH environments [23]. Recent study indicated that TMC nanoparticles are potential carriers for oral protein and vaccine delivery [24]. While the absorption-enhancing effect of TMC is quaternization degree-dependent [25], optimum quaternization degree of 40% was employed in the present work. Moreover, our previous study demonstrated that conjugation of poly (ethylene glycol) (PEG) into chitosan can not only give better solubility, but also reduce the particle sizes of the complexes and improve the stability [13]. Similarly, Kim et al. indicated that hydrophilic PEG chains at the surface of complex induced the maximal compaction of DNA and prevented aggregation of neutralized complexes [26]. Moreover, it was discovered that PEG grafting onto the polymer chain enabled to promote the adhesive process of PEGylated-nanoparticles by

Table 1
Properties and characteristics of the polymers and the PECs

| Polymer (kDa) | DD (%)[a] | Theoretical Mw (kDa)[b] | Determined Mw (kDa)[c] | Substitution | TMC content [% (w/w)] | Mass ratio[d] | Particle size (nm) | Zeta potential (mV) | Drug loading (%) |
|---|---|---|---|---|---|---|---|---|---|
| CS 400 | 85.1% | 400 | 402.2 | | | 2:1 | 697.2 ± 17.6 | 7.5 ± 1.2 | 92.5 ± 2.1 |
| CS 100 | 85.4% | 100 | 109.1 | | | 2:1 | 441.2 ± 10.6 | 7.0 ± 1.6 | 91.5 ± 1.7 |
| CS 50 | 89.9% | 50 | 56.3 | | | 2:1 | 287.9 ± 11.5 | 5.2 ± 0.2 | 93.6 ± 1.5 |
| CS 10 | 85.2% | 10 | 12.5 | | | 2:1 | 233.1 ± 7.2 | 4.7 ± 0.3 | 92.2 ± 0.9 |
| CS(50)-Cys-L | | 50 | | 49.5[e] | | 2:1 | 312.3 ± 5.3 | 3.8 ± 0.7 | 88.9 ± 2.1 |
| CS(50)-Cys-H | | 50 | | 151.2[e] | | 2:1 | 325.5 ± 7.6 | 2.9 ± 0.5 | 87.6 ± 1.9 |
| TMC 50 | | 50 | | 39.0[f] | 100 | 0.3:1 | 195.6 ± 4.2 | 10.5 ± 0.9 | 91.2 ± 1.1 |
| $PEG(5)_{19}$-g-TMC(50) | | 145 | | 6.1[g] | 34.2 ± 0.9 | 1:1 | 178.3 ± 3.6 | 8.3 ± 0.7 | 92.1 ± 2.0 |

[a] DD degree of deacetylation, calculated by $^1$H NMR analysis.
[b] Calculation based on the composition of the copolymer.
[c] Capillary viscosimetry.
[d] Calculation based on the optimized stoichiometric ratio.
[e] Thiol group content (μmol/g), measured by iodine titration.
[f] Degree of quaternization (%).
[g] Calculation based on the primary amino group content in chitosan (%).

interpenetration to the mucosa [27]. Therefore, PEGylated trimethyl chitosan was synthesized to investigate the influence of polymer structure on the properties of the nanocomplexes. Properties of the chitosan derivatives employed in the present study are listed in Table 1.

### 3.2. Effect of system pH

The effects of pH on PEC formation have previously been discussed, with increased pH values promoting the formation of protein–polycation complexes [28]. Since complex formation between proteins and polyelectrolytes is primarily driven by coulombic interactions, the pH of the chitosan solution will influence its charge density and therefore the properties of the resulting PECs. Sato et al. compared the transfection efficiency of DNA/chitosan complexes in A549 cells between pH 6.9 and 7.6. The results indicated that the transfection efficiency was much higher at pH 6.9 than that at pH 7.6 [29].

Influence of system pH on the properties of PECs was investigated by adding enoxaparin solution (0.5 mg/mL) into equal volume (1 mL) of chitosan solutions (1 mg/mL) of different pH values under gentle magnetic stirring. To form PEC, both polymers have to be ionized and bear opposite charges [30], that is to say, the reaction can only be proceeded at pH values in the vicinity of the $pK_a$ interval of the two polymers (the $pK_a$ of heparin is approximately 3.1 [31] and the $pK_a$ of chitosan is approximately 6.5). Consequently, the investigation was carried out mainly in the pH range of 3–7 for chitosan. As depicted in Fig. 1, the particle size of PEC is dependent on both the pH of chitosan solution and chitosan molecular weight. The particle size decreased with increasing pH in the initial stage (pH 3.0–4.5) and a plateau phase was obtained in the pH range of 4.5–6.5, thereafter, the particle size started to increase and particle aggregation was observed above pH 7.0. This can probably be attributed to the fact that in acidic medium, chitosan is highly positively charged and the mutual

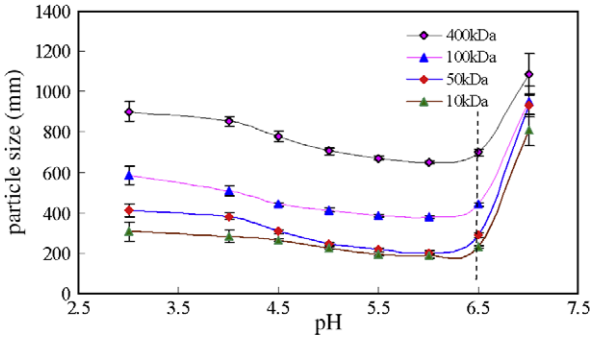


Fig. 1. Relationship between system pH value and particle size for different MW chitosans.

repulsion of the free ammonium groups caused a highly stretched structure of chitosan, forming larger complex with negatively charged enoxaparin. Along with the increase of the system pH, the repulsion force decreased and it facilitated the formation of compact particles with smaller size. However, when the system pH was higher than 6.5, less than 50% of the amino groups of chitosan are positively charged which weakens both the solubility of CS and electrostatic repulsion between particles. The system became instable and tended to coacervate or even precipitate at pH above 7.0.

A similar behavior was observed for the chitosan derivatives but the precipitation pH varied with polymer structure. It was measured to be approximately 7.0, 9.0 and 10.0 for chitosan–cysteine conjugates, TMC and PEGylated TMC, respectively, which can be explained by the different structure properties of the polymers. Unmodified chitosan is only soluble in the acidic environment, in contrast, the solubility of TMC can be guaranteed at pH values above 7, which makes the PEC soluble over a wider pH range (3–9). PEGylated TMC copolymers show even better solubility, which enables the PEC soluble in the pH range of 3–10. In contrast, for chitosan–cysteine conju-

gates, the presence of sulfur groups did not change the solubility significantly and therefore had a similar PEC soluble pH range (3–6.5) as that of the unmodified chitosan. Therefore, the system pH should be below the critical precipitation pH in order to obtain soluble PECs. System pH 6.5 was selected for the following study with the consideration of peroral administration.

### 3.3. Stoichiometric ratio of enoxaparin and chitosan derivatives in PEC

It is well known that polymer/protein ratio has significant influence on the properties of PEC. Therefore, the stoichiometry was investigated in greater detail using dynamic light scattering at pH 6.5. Enoxaparin solutions were titrated against chitosan, and the resulting particle size and Kcps values were measured. The points at which particle size began to increase dramatically, and the Kcps values reached a plateau were denoted as the endpoint of the titration, and the optimal polymer/enoxaparin mass ratio was calculated. Differently structured polymers, namely chitosan 400, 100, 50, 10 kDa, TMC 50 kDa, $PEG(5k)_{19}$-g-TMC(50), and chitosan–cysteine 50 kDa, were investigated under identical conditions. Fig. 2 presents titration data of chitosan 50 kDa/enoxaparin complex.

During the initial stage of titration, large particles were observed, perhaps one enoxaparin molecule linked to a large number of CS molecules as random linkages. Then the mean particle size decreased to a plateau accompanied by a significant Kcps increase, implying the formation of more particles. They condensed to a more defined structure with increasing enoxaparin concentration until a critical point was reached, from where the particle size increased abruptly and the Kcps values kept constant. Therefore, this critical point was selected to calculate the optimal mass ratio between chitosan and enoxaparin (2:1). After this critical point, flocculation occurred shortly due to the significantly increased particle size.

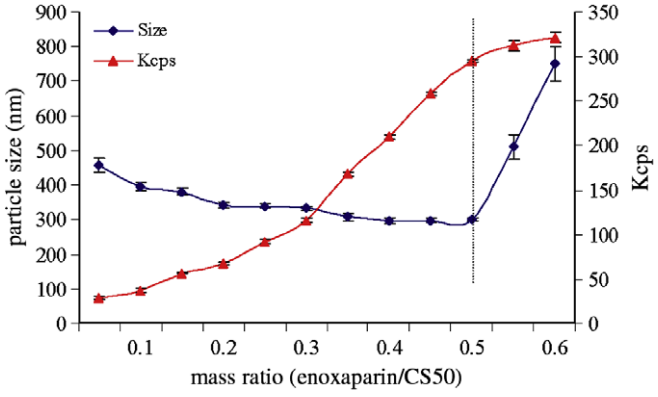


Fig. 2. Evolution of particle size and Kcps values of chitosan 50 kDa–enoxaparin complex versus enoxaparin/chitosan mass ratio. (♦) Size; (▲) Kcps. Particle size and Kcps values of the PEC were monitored by dynamic light scattering.

It is noteworthy that the stoichiometric ratio was found to be polymer structure-dependent. As listed in Table 1, the optimal mass ratio was approximately 2:1, 0.3:1, 1:1 for chitosan–cysteine 50 kDa, TMC 50 kDa, and $PEG(5)_{19}$-g-TMC(50), respectively. This suggests that the stoichiometry of the complexes is primarily determined by the charge density of the polymers, which is in the order of TMC 50 kDa > $PEG(5)_{19}$-g-TMC(50) > chitosan–cysteine 50 kDa due to the structure modification as described in Section 3.2.

### 3.4. Effect of polymer molecular weight and concentration

Since all interpolymer interactions are known to be critically dependent on the chain lengths of the interacting macromolecules, enoxaparin nanocomplexes were prepared with different molecular weight chitosans at the optimized stoichiometric ratio and the properties are listed in Table 1. The particle size of CS/enoxaparin complexes was obviously chitosan MW-dependent and decreased significantly when CS MW decreased from 400 kDa to 10 kDa ($p < 0.05$). This may be explained by the fact that at the same mass ratio, a decrease in molecular weight means a higher number of macromolecular coils, therefore more cationic groups will be exposed at the outer parts and facilitate formation and compaction of the complexes. However, no statistical differences in particle size were observed between chitosan 50 kDa and chitosan 10 kDa ($p > 0.05$). In addition, the complexes displayed a slight decrease in surface charge with the decrease of chitosan molecular weight, with a zeta potential value of $4.7 \pm 0.3$ versus $7.5 \pm 1.2$ for chitosan 10 kDa and chitosan 400 kDa, respectively. However, no statistical difference in drug loading was found with different MW chitosans.

Properties of the nanocomplexes were also polymer concentration dependent. As shown in Fig. 3, particle size of the PECs increased with increasing chitosan concentration irrespective of MW (for chitosan 50 kDa, $232.1 \pm 5.8$ nm at 0.5 mg/mL compared to $811.6 \pm 35.3$ nm at 3 mg/mL). This phenomenon can probably be explained by the fact that, while chitosan/enoxaparin mass ratio was constant, increasing polymer concentration will increase the number

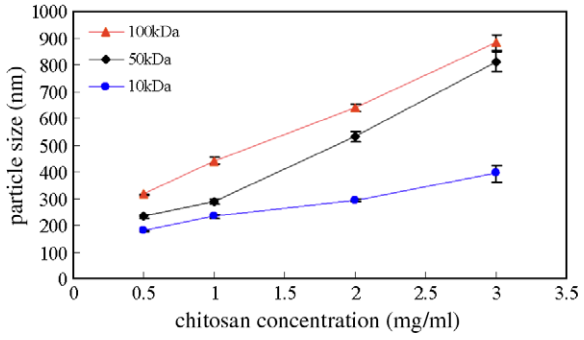


Fig. 3. Effect of polymer concentration on the formation of enoxaparin complexes with different MW chitosans (system pH 6.5, mass ratio CS/enoxaparin 2/1).

of the nanocomplexes formed in the system, leading to an increased aggregation tendency. On the other hand, it is also possible that one heparin molecular reacted with more than one chitosan molecular, causing increased particle size. However, the rate of particle-size increase was found to be chitosan MW-dependent, which were 223.5, 236.9, 82.6 for chitosan 100, 50 and 10 kDa, respectively, indicating that the particle size of PEC was less sensible to polymer concentration change with low MW chitosan (10 kDa) compared to that of high MW chitosans (>50 kDa).

### 3.5. Effect of polymer structure

The chemical modification of chitosan is expected to change physicochemical properties of the PECs. Taking chitosan 50 kDa for example, effects of polymer structure on the physicochemical properties of the PECs were investigated. Table 1 summarizes the characteristics of the PECs based on various chitosan derivatives.

The particle size of PECs prepared with TMC 50 and PEGylated TMC 50 kDa copolymers was significantly smaller than that prepared with unmodified chitosan ($p < 0.05$), which can be explained by the stronger ionic interactions with enoxaparin. Compared with the homopolymer TMC, PEGylated TMC copolymer caused a further decrease in particle size ($p < 0.05$), suggesting that the hydrophilic PEG chains promoted complex condensation. In contrast, the particle size of the PECs formed with the thiolated chitosans increased with the increase of thiolation degree ($p < 0.05$), which can be explained by the decreased charge density due to amino group substitution. Similar results were reported by Bravo-Osuna et al. [15]. However, when we increased thiol-group content from 49.5 to 151.2 μmol/g, there was only slight increase in particle size, 312.3 ± 5.3 nm versus 325.5 ± 7.6 nm.

Zeta potentials of the PECs at stoichiometric ratios were measured and are listed in Table 1. All of the PECs are positively charged, and the charge values are in the order of TMC 50 kDa > $PEG(5)_{19}$-g-TMC(50) > chitosan 50 kDa > chitosan–cysteine 50 kDa. PECs based on TMC 50 and PEGylated TMC 50 kDa copolymers showed significantly higher zeta potentials than that of chitosan 50 kDa ($p < 0.05$), which could be explained by the increased number of positive charges on the polymer chains. The PEGylated copolymer showed a reduced zeta potential compared with TMC ($p < 0.05$), indicating the shielding effect of PEG chains. Additionally, the zeta potential decreased slightly with increasing the thiol-group content, while thiolation of the polymer changes the amount of amino groups available in the polymer structure. On the other hand, the positive charge of the PEC implies that heparin was encapsulated in the chitosan chains, which projected their positively charged chains toward the external aqueous medium, ensuring the electrostatic interactions with the anionic groups of the mucus and facilitating heparin uptake.

While heparin is a highly negatively charged molecule, consequently, it was expected to interact with chitosan very efficiently. As anticipated, the association efficiencies of enoxaparin in PECs were considerably high, at approximately 90%, regardless of polymer structure. It was noticed that the association efficiencies of the PEC prepared with thiolated chitosans decreased slightly due to the decreased charge density as explained previously. However, no statistical difference in association efficiency was observed at two different degrees of thiolation ($p > 0.05$).

### 3.6. Complex stability

Since the electrostatic attraction between the cationic amino groups of chitosan and the anionic groups of enoxaparin is the main interaction leading to the formation of PEC, the ionic strength of the system was expected to strongly influence the stability of PEC. The electrostatic attraction could be weakened by the addition of salts, such as NaCl, while their presence reduces the attraction between the oppositely charged polyelectrolytes by contributing to the counter-ion environment [30].

In order to investigate the effect of salt on the chitosan–enoxaparin interaction, the ionic strength of the solution was adjusted by adding NaCl. This was achieved by mixing various PECs with a series of concentrated NaCl solutions, and monitoring the integrity of the PECs immediately after mixing by dynamic light scattering. Since we found no apparent change in particle size, only the evolution of Kcps values are noted and compared. The degree of influence was polymer structure-dependent. The PECs of chitosan 50 kDa were stable at ionic strength $\leqslant$75 mM, significant decrease in Kcps value was observed at ionic strength $\geqslant$150 mM, indicating complex dissociation. For chitosan 50 kDa, a linear relationship between ionic strength ($x$) and remaining kcps percentage ($y$) was established with the equation $y = -0.079x + 102.54$ ($n = 5$, $r = 0.994$). This phenomenon demonstrated that the interactions involved in PEC formation were partly electrostatic. However, the PECs of chitosan derivatives were rather stable against ionic strength even when ionic strength was as high as 300 mM, as a consequence of the steric effect of methyl groups, polyethylene glycol segments and the formation of disulfide bonds for TMC, PEGylated TMC and chitosan–cysteine conjugates, respectively. Moreover, in addition to electrostatic interaction, hydrophobic ionic pairing also contributed to the formation of the PEC [32].

### 3.7. Visualization of the nanocomplexes

Morphology of different PECs was observed with atomic force microscopy (AFM) and is shown in Fig. 4. The particle size obtained from AFM images was much smaller than that obtained from dynamic light scattering (Table 1). In addition to the different measurement mechanism, different sample treatments would easily explain the lower nanocomplex sizes observed by AFM. For the PCS

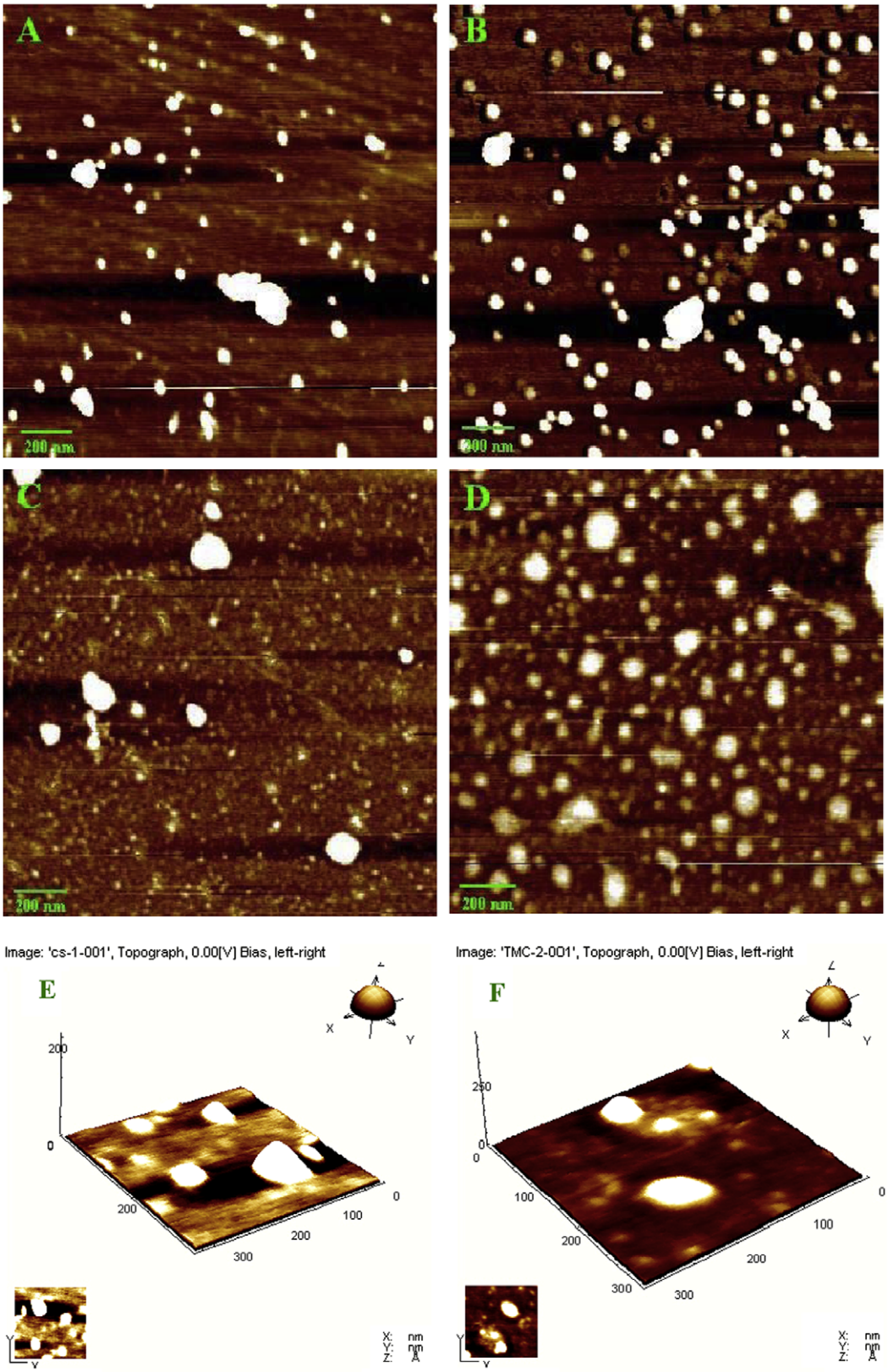


Fig. 4. Atomic force microscopy images of polymer–enoxaparin complexes at optimized mass ratio. (A) Chitosan 50 kDa, (B) chitosan–cysteine conjugates 50 kDa, (C) trimethyl chitosan 50 kDa, (D) PEG(5)$_{19}$-g-TMC(50), (E) three-dimensional image of chitosan 50 kDa, (F) three-dimensional image of trimethyl chitosan 50 kDa.

technique, nanoparticles were suspended in aqueous medium, so the nanocomplexes were well swelled. On the other hand, for AFM measurements, nanocomplexes were previously dried at room temperature, and the nanocomplexes

would shrink under drying. Similar phenomenon has been reported previously [21]. In Fig. 4A, most of the chitosan complexes have an average diameter of 40–50 nm with spherical shape, smooth surface and compacted structure. There are also big particles with size between 100 and 200 nm. The big particles might consist of two or more of the small ones. Similar phenomenon was observed for thiolated chitosans with slight particle size increase, as shown in Fig. 4B. In contrast, extremely small particles were observed for the PECs formed with TMC (Fig. 4C). There were also some aggregates with particle size of 100–200 nm. Compared to other polymers, PECs formed with PEGylated copolymers (Fig. 4D) were rather large, with average particle size of approximately 100 nm. However, it shows that majority of the particles were separated from one another, suggesting that these PECs were possibly stabilized against agglomeration, mainly due to the stabilization effect of hydrophilic PEG chains at the surface of the complex. Three-dimensional images (Fig. 4E and F) further demonstrated that the particles were approximately spherical in shape. In addition, it should be indicated that, while only limited nanocomplexes were measured in AFM, the particle size is not as representative as that from dynamic light scattering method and AFM is mainly used for morphology observation in this study.

## 4. Conclusions

Based on the results presented above, it is reasonable to conclude that the interactions involved in PEC formation are partly electrostatic, also involving other hydrophobic interactions. In the present work, self-assembled enoxaparin PECs were formed with chitosan, chitosan–cysteine conjugates, TMC and PEGylated TMC copolymer. The PEC formation process was influenced by a variety of parameters, including the system pH, polymer/enoxaparin mass ratio, polymer molecular weight, concentration and structure, etc. Soluble nanocomplexes in the size range of 200–500 nm with spherical morphology could be obtained in the pH range of 3.0–6.5, with positive charge and drug encapsulation efficiency of approximately 90%. These studies have contributed much to the understanding of PEC formation and complexation with enoxaparin. This work will be furthered by performing peroral absorption studies in animal models.

## Acknowledgment

This project is financially sponsored by the Scientific Research Foundation for the Returned Overseas Chinese Scholars, State Education Ministry.

## References

[1] J. Hirsh, T. Warkentin, R. Raschke, C. Granger, E. Ohman, J. Dalen, Heparin and low-molecular-weight heparin: mechanisms of action, pharmacokinetics, dosing considerations, monitoring, efficacy, and safety, Chest 114 (1998) 489–510.
[2] Y. Prasad, T. Minamimoto, Y. Yoshikawa, N. Shibata, S. Mori, A. Matsuura, K. Takada, In situ intestinal absorption studies on low molecular weight heparin in rats using Labrasol as absorption enhancer, Int. J. Pharm. 271 (2004) 225–232.
[3] B. Ross, I. Toth, Gastrointestinal absorption of heparin by lipidization or coadministration with penetration enhancers, Curr. Drug Deliv. 2 (2005) 277–287.
[4] T. Schmitz, V. Leitner, A. Bernkop-Schnürch, Oral heparin delivery: design and in vivo evaluation of a stomach-targeted mucoadhesive delivery system, J. Pharm. Sci. 94 (2005) 966–973.
[5] S. Kim, B. Vaishali, E. Lee, S. Lee, Y. Lee, T. Kumar, H. Moon, Y. Byuna, Oral delivery of chemical conjugates of heparin and deoxycholic acid in aqueous formulation, Thromb. Res. 117 (2006) 419–427.
[6] V. Hoffart, A. Lamprecht, P. Maincent, T. Lecompte, C. Vigneron, N. Ubrich, Oral bioavailability of a low molecular weight heparin using a polymeric delivery system, J. Control. Release 113 (2006) 38–42.
[7] S. Mao, U. Bakowsky, A. Jintapattanakit, T. Kissel, Self-assembled polyelectrolyte nanocomplexes between chitosan derivatives and insulin, J. Pharm. Sci. 95 (2006) 1035–1048.
[8] A. Krauland, M. Alonso, Chitosan/cyclodextrin nanoparticles as macromolecular drug delivery system, Int. J. Pharm. 340 (2007) 134–142.
[9] O. Gaserod, I.G. Jolliffe, F.C. Hampson, P.W. Dettmar, G. Skjak-Braek, The enhancement of the bioadhesive properties of calcium alginate gel beads by coating with chitosan, Int. J. Pharm. 175 (1998) 237–246.
[10] L. Illum, I. Jabbal-Gill, M. Hinchcliffe, A.N. Fisher, S.S. Davis, Chitosan as a novel nasal delivery system for vaccines, Adv. Drug Deliv. Rev. 51 (2001) 81–96.
[11] R. Hejazi, M. Amiji, Chitosan-based gastrointestinal delivery systems, J. Control. Release 89 (2003) 151–165.
[12] A. Bernkop-Schnürch, Chitosan and its derivatives: potential excipients for peroral peptide delivery systems, Int. J. Pharm. 194 (2000) 1–13.
[13] S. Mao, X. Shuai, F. Unger, M. Wittmar, X. Xie, T. Kissel, Synthesis, characterization and cytotoxicity of poly(ethylene glycol)-graft-trimethyl chitosan block copolymer, Biomaterials 26 (2005) 6343–6356.
[14] S. Mao, O. Germershaus, D. Fischer, T. Linn, R. Schnepf, T. Kissel, Uptake and transport of PEG-graft-trimethyl-chitosan copolymer-insulin nanocomplexes by epithelial cells, Pharm. Res. 22 (2005) 2058–2068.
[15] I. Bravo-Osuna, T. Schmitz, A. Bernkop-Schnürch, C. Vauthier, G. Ponchel, Elaboration and characterization of thiolated chitosan-coated acrylic nanoparticles, Int. J. Pharm. 316 (2006) 170–175.
[16] Y. Kikuchi, Polyelectrolyte complex of heparin with chitosan, Makromol. Chem. 175 (1974) 2209–2211.
[17] S. Mao, X. Shuai, F. Unger, M. Simon, D. Bi, T. Kissel, The depolymerization of chitosan: effects on physicochemical and biological properties, Int. J. Pharm. 281 (2004) 45–54.
[18] A.B. Sieval, M. Thanou, A.F. Kotze, J.C. Verhoef, J. Brussee, H.E. Junginger, Preparation and NMR characterization of highly substituted *N*-trimethyl chitosan chloride, Carbohydr. Polym. 36 (1998) 157–165.
[19] A. Bernkop-Schnürch, M. Hornof, D. Guggi, Thiolated chitosans, Eur. J. Pharm. Biopharm. 57 (2004) 9–17.
[20] Y. Jiao, N. Ubrich, M. Marchand-Arvier, C. Vigneron, M. Hoffman, T. Lecompte, P. Maincent, In vitro and in vivo evaluation of oral heparin-loaded polymeric nanoparticles in rabbits, Circulation 105 (2002) 230–235.
[21] I. Bravo-Osuna, G. Ponchel, C. Vauthier, Tuning of shell and core characteristics of chitosan-decorated acrylic nanoparticles, Eur. J. Pharm. Sci. 30 (2007) 143–154.
[22] A. Bernkop-Schnürch, Thiomers: a new generation of mucoadhesive polymers, Adv. Drug Deliv. Rev. 57 (2005) 1569–1582.

[23] S.M. van der Merwe, J.C. Verhoef, J.H.M. Verheijden, A.F. Kotze, H.E. Junginger, Trimethylated chitosan as polymeric absorption enhancer for improved peroral delivery of peptide drugs, Eur. J. Pharm. Biopharm. 58 (2004) 225–235.
[24] F. Chen, Z. Zhang, F. Yuan, X. Qin, M. Wang, Y. Huang, In vitro and in vivo study of *N*-trimethyl chitosan nanoparticles for oral protein delivery, Int. J. Pharm. 349 (2008) 226–233.
[25] J.H. Hamman, C.M. Schultz, A.F. Kotze, *N*-Trimethyl chitosan chloride: optimum degree of quaternization for drug absorption enhancement across epithelial cells, Drug Dev. Ind. Pharm. 29 (2003) 161–172.
[26] T. Kim, H. Jiang, D. Jere, I. Park, M. Cho, J. Nah, Y. Choi, T. Akaike, C. Cho, Chemical modification of chitosan as a gene carrier in vitro and in vivo, Prog. Polym. Sci. 32 (2007) 726–753.
[27] L. Serra, J. Domenech, N.A. Peppas, Design of poly(ethylene glycol)-tethered copolymers as novel mucoadhesive drug delivery systems, Eur. J. Pharm. Biopharm. 63 (2006) 11–18.
[28] J.M. Park, B.B. Muhoberac, P.L. Dubin, J. Xia, Effects of protein charge heterogeneity in protein-polyelectrolyte complexation, Macromolecules 25 (1992) 290–295.
[29] T. Sato, T. Ishii, Y. Okahata, In vitro gene delivery mediated by chitosan. Effect of pH, serum, and molecular mass of chitosan on the transfection efficiency, Biomaterials 22 (2001) 2075–2080.
[30] J. Berger, M. Reist, J.M. Mayer, O. Felt, R. Gurny, Structure and interactions in chitosan hydrogels formed by complexation or aggregation for biomedical applications, Eur. J. Pharm. Biopharm. 57 (2004) 35–52.
[31] H. Wang, D. Loganathan, R. Linhardt, Determination of the p$K_a$ of glucuronic acid and the carboxy groups of heparin by carbon-13 nuclear magnetic resonance spectroscopy, Biochem. J. 278 (1991) 689–695.
[32] D. Quintanar-Guerrero, E. Allemann, H. Fessi, E. Doelker, Applications of the ion-pair concept to hydrophilic substances with special emphasis on peptides, Pharm. Res. 14 (1997) 119–127.